July 1974 LRP 85/74

EXPERIMENTAL AND COMPUTATIONAL STUDY OF THE LOW-DENSITY PLASMA IN THE OUTER REGIONS OF A THETA PINCH

P. Hafner and F. Hofmann

Centre de Recherches en Physique des Plasmas

ECOLE POLYTECHNIQUE FEDERALE DE LAUSANNE

July 1974 LRP 85/74

EXPERIMENTAL AND COMPUTATIONAL SUTDY OF THE LOW-DENSITY PLASMA IN THE OUTER REGIONS OF A THETA PINCH

P. Hafner and F. Hofmann

E R R A T A

Page 20, figure 11: the radius R should be given in "cm" and not in "mm".

July 1974

LRP 85/74

EXPERIMENTAL AND COMPUTATIONAL STUDY OF THE LOW-DENSITY PLASMA IN THE OUTER REGIONS OF A THETA PINCH

P. Hafner and F. Hofmann

A b s t r a c t

The time evolution of the electron density has been measured in the outer regions of a fast theta pinch by means of a Mach-Zehnder interferometer. The results show that the electron density outside the central plasma column is relatively high, i.e. between 1 and $5 * 10^{14}$ cm^{-3}. A comparison of these measurements with theoretical calculations leads to the conclusion that the pinch must be unstable during the implosion phase.

1. INTRODUCTION

While the presence of low-density plasma in the outer regions of theta pinches has been known for some time, the origin and the properties of this plasma are still largely unknown. Yet, the low-density plasma is crucially important in high-beta CTR experiments for the following reasons: First, the success of feedback stabilization of toroidal pinches [1] depends, to a large extent, on the electrical properties of the dilute plasma surrounding the dense core. Second, particle and energy confinement times, as well as contamination and cooling by impurities from the wall, are strongly influenced by the plasma parameters in the outer regions.

It has been shown [2] that the electron density in the dilute plasma is much higher than that expected from classical MHD theory. The discrepancy has been attributed, in the past, to a number of different phenomena, such as anomalous diffusion [2], flute instabilities [3], ionization of neutral gas [4], etc.

In order to shed some light onto these questions, we have measured the electron density in the outer regions of a theta pinch, and we have simulated the experiment on a computer, using a one-dimensional, three-fluid MHD code.

2. EXPERIMENTAL APPARATUS

The measurements reported in this paper were made on a new installation, the "Lausanne Linear Theta Pinch". A schematic diagram of the experimental apparatus is shown in Fig. 1. A 120 kJ capacitor bank feeds a single turn compression coil, and the plasma is produced in a quartz discharge tube. The capacitor bank was designed and built by Culham Laboratory. It consists of eight 18.8 μF capacitors, connected in parallel. Each capacitor is switched by its own pressurized air spark gap. Since the system has no crowbar switch, a resistor had to be connected in series with the load, in order to reduce the amount of voltage reversal to a tolerable level. This was achieved by using stainless

steel connecting plates between the bank output and the coil. The basic parameters of the apparatus are listed in the Table, below:

Length of coil	100 cm
Inner diameter of coil	12 cm
Length of quartz discharge tube	160 cm
Inner diameter of discharge tube	10 cm
Bank capacitance	150 μF
Bank inductance	8.4 nH
Total inductance	24.9 nH
Quarter period	3.0 μs
Bank charging voltage	35 kV
Maximum magnetic field	30 kG
Maximum rate of change of magnetic field	1.57×10^{10} G/s

Special care has been taken to reduce the impurity content in the discharge to an absolute minimum. The vacuum pump is isolated from the discharge tube by a liquid nitrogen trap. Indium O-rings and molybdenum electrodes are used throughout the system. In addition, the diameter of the quartz tube is enlarged, just outside the coil, in order to avoid contamination by plasma bombardment of the tube wall (see Fig. 1).

Deuterium gas was used for all experiments described here. The gas was preionized by a fast axial current pulse of 13 kA peak current and 2 μs duration. This type of preionization [5,6,7] minimizes plasma-wall contact and impurity concentrations in the discharge. The preionization circuit is driven by a small capacitor bank (0.2 μF), charged to 50 kV. Non-linear resistors are used to damp out the current after one half-period (Fig. 2). The preionization discharge is initiated by a small trigger spark at the cathode. This trigger spark reduces the time jitter, makes the discharge very reproducible, and allows reliable breakdown at filling pressures down to 5 mTorr (see Figs. 3 and 4).

The main θ-pinch discharge is triggered 1 μs after the end of the preionization pulse (Fig. 2). At this time, the axial current through the plasma is negligibly small.

3. MEASUREMENTS

3.1 Streak Photography

Stereoscopic streak photographs were taken through radial slits in the compression coil (Figs. 5 and 6). The slits are located at the midplane of the coil (see Fig. 1). On each photograph, the upper view shows the radial motion of the plasma column in the horizontal plane, whereas the lower view shows the radial motion in the vertical plane. A slow drift of the plasma column towards the collector was originally observed (Fig. 5). It was found that this drift was caused by image currents in the mechanical support structure for the collector plates. The drift could be suppressed almost completely by mounting an aluminum plate, having the same dimensions as the collector support structure, on the opposite side of the coil (Fig. 6). Note that the plasma column is grossly stable and remains in the center of the discharge tube throughout the duration of the experiment (4 μs).

The total mass collected by the implosion can be deduced [8] from the frequency of the radial, hydromagnetic oscillations of the plasma column, as observed on streak photographs. This frequency is given by

$$\omega = g\sqrt{\frac{B^2}{M}}$$

where B is the magnetic field in Gauss, M is the plasma line mass in gr cm^{-1}, and g is a correction factor depending on the radial density profile [10]. If we assume M constant in time and g = 1.2 [9], we obtain the following

results:

filling pressure	M/M_o
20 mTorr D_2	0.73 ± 0.15
40 mTorr D_2	0.52 ± 0.10

Here, M_o is the line mass corresponding to the initial filling density. The relatively poor collection efficiency is a phenomenon that is commonly observed in θ-pinches. It cannot be explained by the fact that the plasma is partially ionized at the beginning of the implosion, because the passage of the shock wave produces virtually complete ionization. The poor collection efficiency is probably due to an instability during the implosion phase of the pinch, as will be shown in the following sections.

3.2 Electron density

Electron densities were measured by means of a Mach-Zehnder interferometer [10], using a He-Ne laser. The laser beam traverses the plasma parallel to the discharge tube axis. The time variation of the electron density, integrated along the path of the laser beam, is measured with the beam located at a fixed radial position. Density profiles are then obtained by repeating the measurement at a number of radial positions. The sensitivity of the instrument is limited by photomultiplier noise to about 0.01 fringes. This corresponds to a minimum measurable density of 5×10^{13} cm^{-3}.

Great care has been taken in this measurement to eliminate possible sources of error, especially end effects. The He-Ne laser beam passes through thin quartz tubes, so-called "look-ins", extending up to the edge of the coil, such that any electrons that may be present outside the coil do not influence the measurement.

Fig. 7 shows the time evolution of the electron density, at a fixed radial position. The measurements were done, using two different kinds of look-ins. In case (a), alumina look-ins having a large rectangular cross-section were used. These look-ins produced considerable contamination of the discharge, as a result of plasma bombardment of their surfaces. The effect can be seen in Fig. 7, which shows that the electron density increases during the latter part of the experiment in spite of rapid plasma loss through the ends of the tube.

In case (b), the contamination has been eliminated by the use of quartz look-ins having a very small circular cross section, as shown in Fig. 7.

Figs. 8 and 9 show the time dependence of the electron density at differents radial positions.

Fig. 10 shows the time evolution of the electron density profile $n_e(r)$. Immediately after the first implosion (0.6 μs), the central column is surrounded by low-density plasma. The electron density decreases with increasing radius from about 2×10^{15} cm^{-3} at r = 18 mm to about 5×10^{13} cm^{-3} at r = 46 mm. The density profile in the outer region then remains almost constant in time, up to maximum compression (3 μs). In contrast to previous measurements [11], our radial density profiles do not show a maximum in the outer region.

3.3 Temperature

The plasma temperature was not measured in this experiment, but a rough estimate can be obtained from the measured line mass and an assumed beta-value. At 20 mTorr D_2 filling pressure and at t = 3 μs (maximum field), the radius of the plasma column, as observed on streak photographs, is approximately 0.8 cm. The line mass, deduced from the radial bounce oscillations, is equal to 2.5×10^{-7} g/cm. Consequently, the average number density in the central column is approximately 3.8×10^{16} cm^{-3}. Assuming $\beta = 0.8$ (a reasonable value for this kind of pinch), we obtain for the sum of the electron and ion temperatures, $kT_e + kT_i = 480$ eV.

4. THEORY

The theta pinch was simulated on a computer, using a one-dimensional MHD code [12] . The code is based on a three-fluid model of a partially ionized plasma, consisting of electrons, ions and neutral atoms. The model includes the effects of ionization, recombination, resistivity, viscosity, thermal conductivity and ion neutral collisions. Plasma initial conditions and magnetic field boundary conditions at the wall were taken as measured in the experiment. The only adjustable parameters in the calculation were the resistivity (classical or various kinds of anomalous resistivity) and a flux of plasma from the wall which simulates degassing. Fig. 11 shows the comparison between measurements and calculations. If one assumes classical resistivity and zero flux from the wall, the computed electron density in the outer region is almost two orders of magnitude less than the measured one. Introducing a plasma flux from the wall obviously increases the density in the outer region, but produces a density gradient whose sign is opposite to the measured one. Anomalous resistivity gives rise to enhanced diffusion of plasma from the central column and, thus, also produces additional density in the outer region. However, we found that none of the currently available prescriptions for anomalous resistivity was successful in reproducing the measured density profiles at early times.

5. CONCLUSION

Comparison between measurements in a theta pinch and numerical simulation has shown that the measured electron density in the outer regions is much higher than the computed one. This is especially true at early times, just after the first implosion. Effects such as anomalous diffusion, ionization of neutral gas by electron impact and degassing of the walls were taken into account in the theoretical model. These phonemena cannot explain the discrepancy between theory and experiment. Other physical processes, which are not included in our theory, such as ionization of neutral gas by fast neutral atoms and photoionization, can easily be shown to be negligible

in our case. Having thus ruled out virtually all microscopic processes, we are led to the conclusion that we must be dealing with a macroscopic phenomenon, i.e., an instability during the implosion phase of the pinch. This would give rise to a breakup of the field-plasma interface and, hence, an incomplete plasma collection. Such instabilities have actually been observed in particle-in-cell calculations [13] of the early phase of a theta pinch.

Acknowledgements

The authors wish to thank Dr. A. Heym for many fruitful discussions. They acknowledge the technical assistance of K. Hruska, H. Ripper, A. Simik, J.P. Rouyet, L. Hafner and G. du Crest.

This work was supported by the "Fonds National Suisse de la Recherche Scientifique".

Figure Captions

Fig. 1 Schematic diagram of the experimental apparatus.

Fig. 2 Time sequence of preionization current (lower trace) and θ-pinch current (upper trace). The time scale is 1.0 μs per division.

Fig. 3 Voltage on the cathode (left) and preionization current (right) at a filling pressure of 5 mTorr D_2. The preionization discharge was initiated by a trigger spark at the cathode. Time scale: 2 μs per division, 5 discharges superimposed.

Fig. 4 Cathode voltage (left) and preionization current (right), at a filling pressure of 10 mTorr D_2, (a): without trigger spark, 5 discharges superimposed, and (b): with trigger spark, 15 discharges superimposed. Time scale: 2 μs per division. The overshoot in the preionization current was due to the fact that the nonlinear resistors were not properly adjusted. This could easily be eliminated, as seen in Fig. 2.

Fig. 5 Stereoscopic streak photographs of the discharge, at filling pressures of 20 and 40 mTorr D_2. The time dependence of the magnetic field is shown in the lower half of the figure.

Fig. 6 Stereoscopic streak photographs of the discharge, at filling pressures of 20 and 40 mTorr D_2, after mounting an aluminum plate which compensates image currents in the collector support structure.

Fig. 7 Time evolution of the electron density measured at a fixed radial position, r = 36 mm, with two different kinds of "look-ins".

Fig. 8 Measured electron density, as a function of time, at various radial positions (r = 18 to r = 28 mm).

Fig. 9 Measured electron density, as a function of time, at various radial positions (r = 30 to r = 46 mm).

Fig. 10 Time evolution of the electron density profile $n_e(r)$ at a filling pressure of 20 mTorr D_2.

Fig. 11 Measured and calculated electron density profiles. Measurements are represented by dots. The dashed line shows the computed density, assuming a particle flux from the wall of $4 * 10^{13}$ electron-ion pairs per cm^2 per μs. The solid line shows the result of a similar calculation, assuming a particle flux ten times as large ($4 * 10^{14}$ cm^{-2} μs^{-1}). In both calculations a Bohm-type anomalous resistivity has been used.

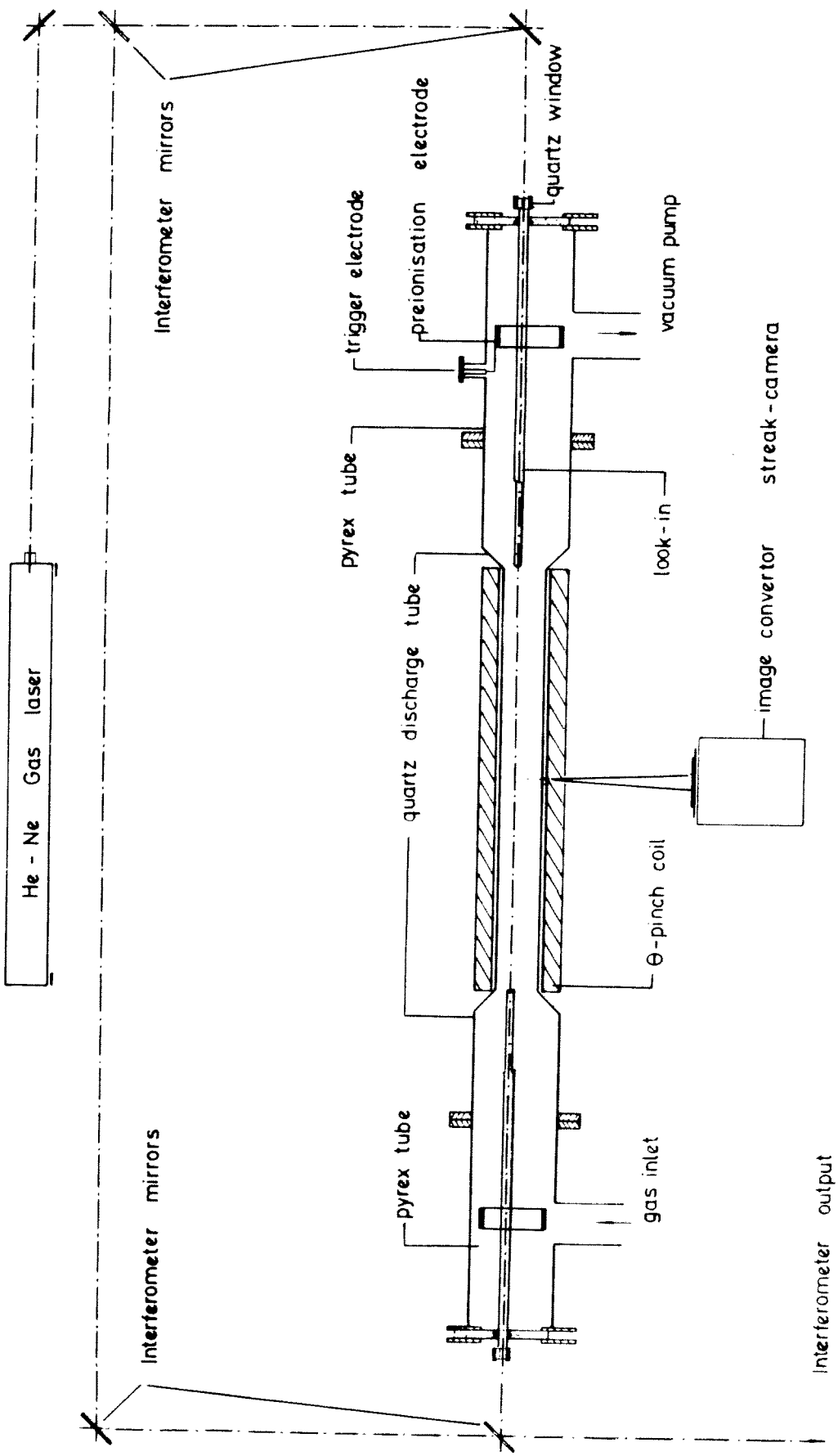
He - Ne Gas laser
Interferometer mirrors
trigger electrode
preionisation electrode
quartz window
vacuum pump
Pyrex tube
look-in
streak-camera
quartz discharge tube
image convertor
θ-pinch coil
pyrex tube
gas inlet
Interferometer mirrors
Interferometer output

Figure 1

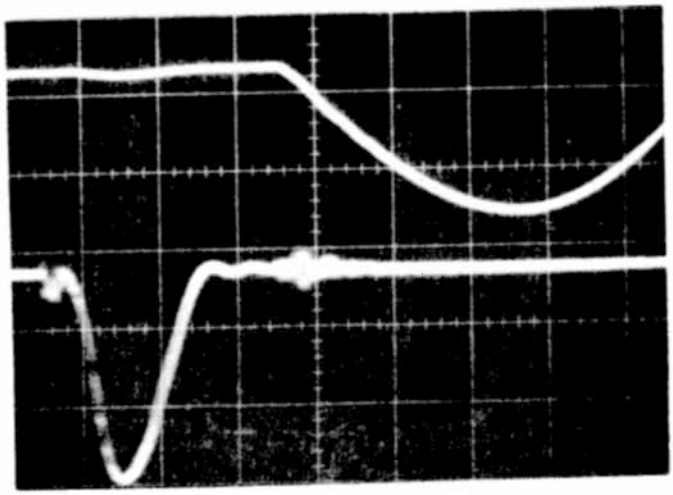

Figure 2

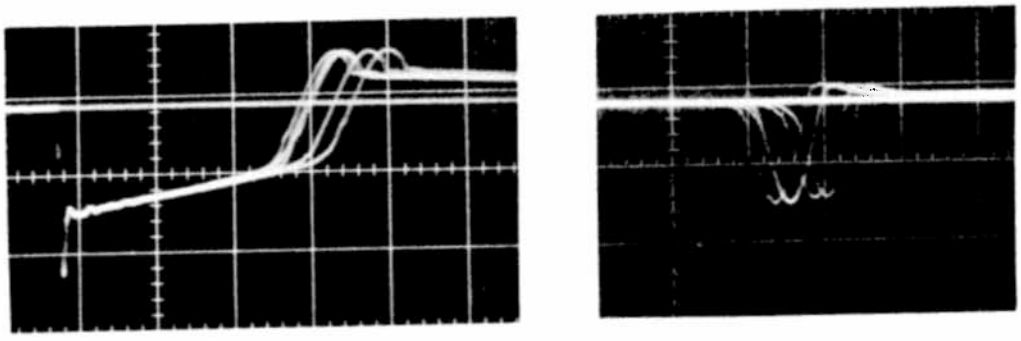

Figure 3

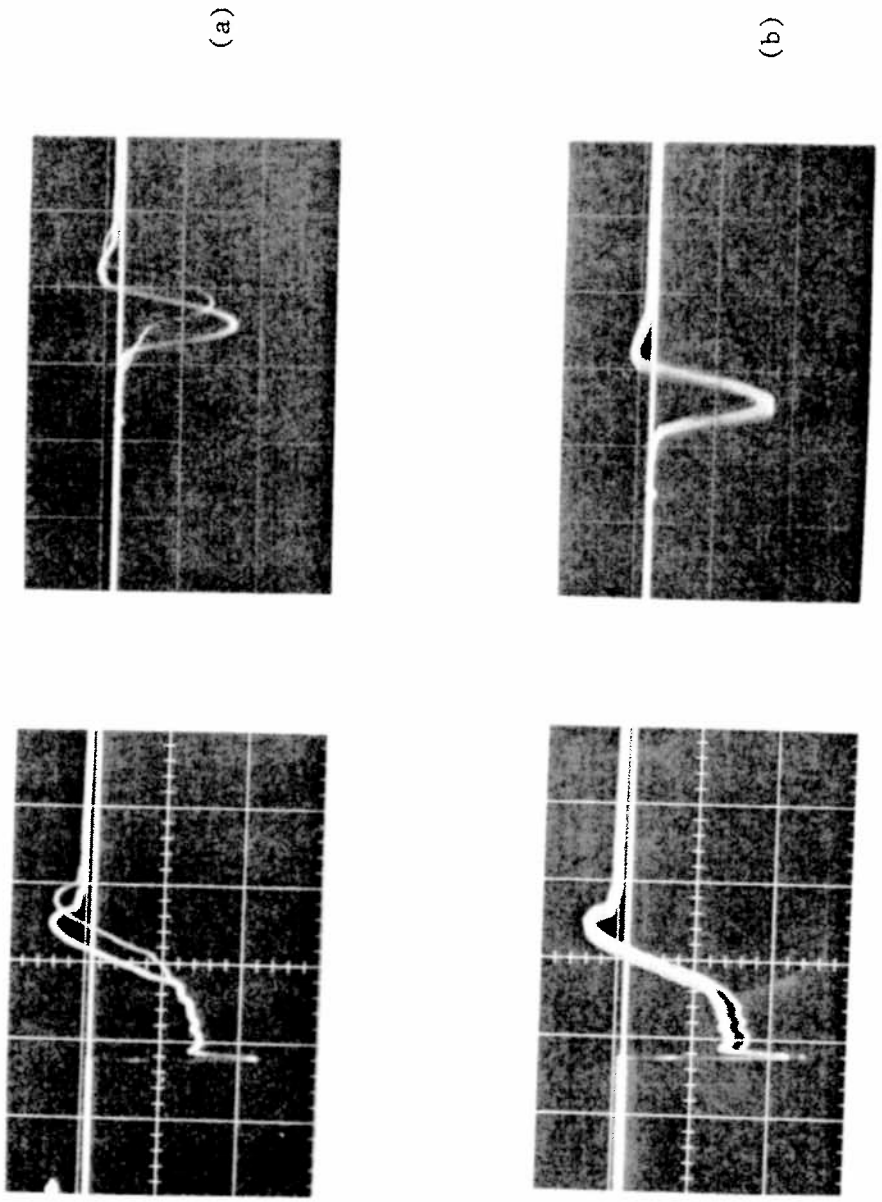

Figure 4

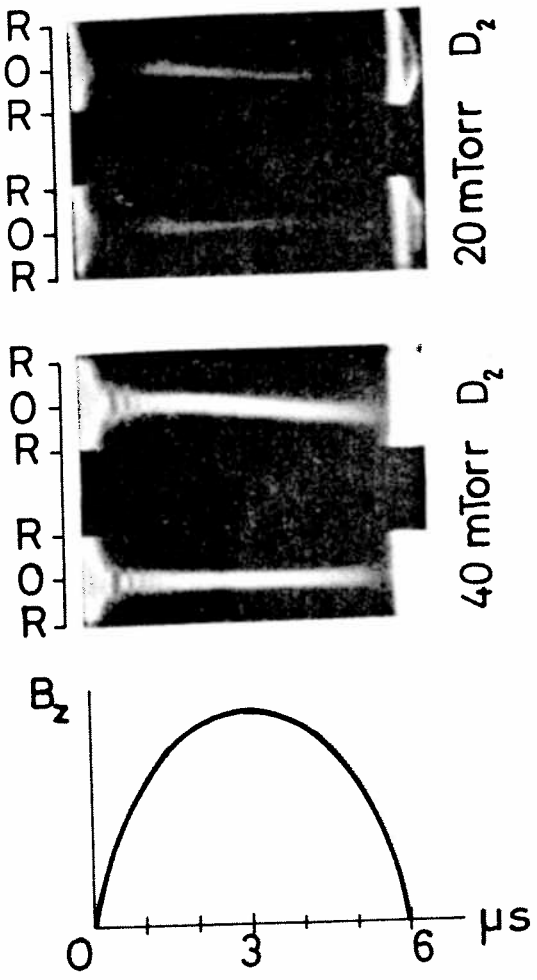

Figure 5

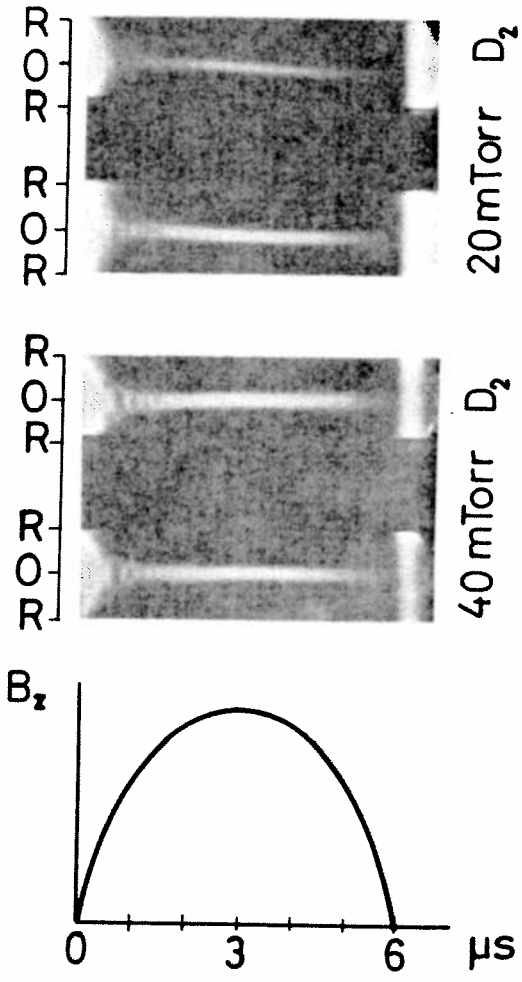

Figure 6

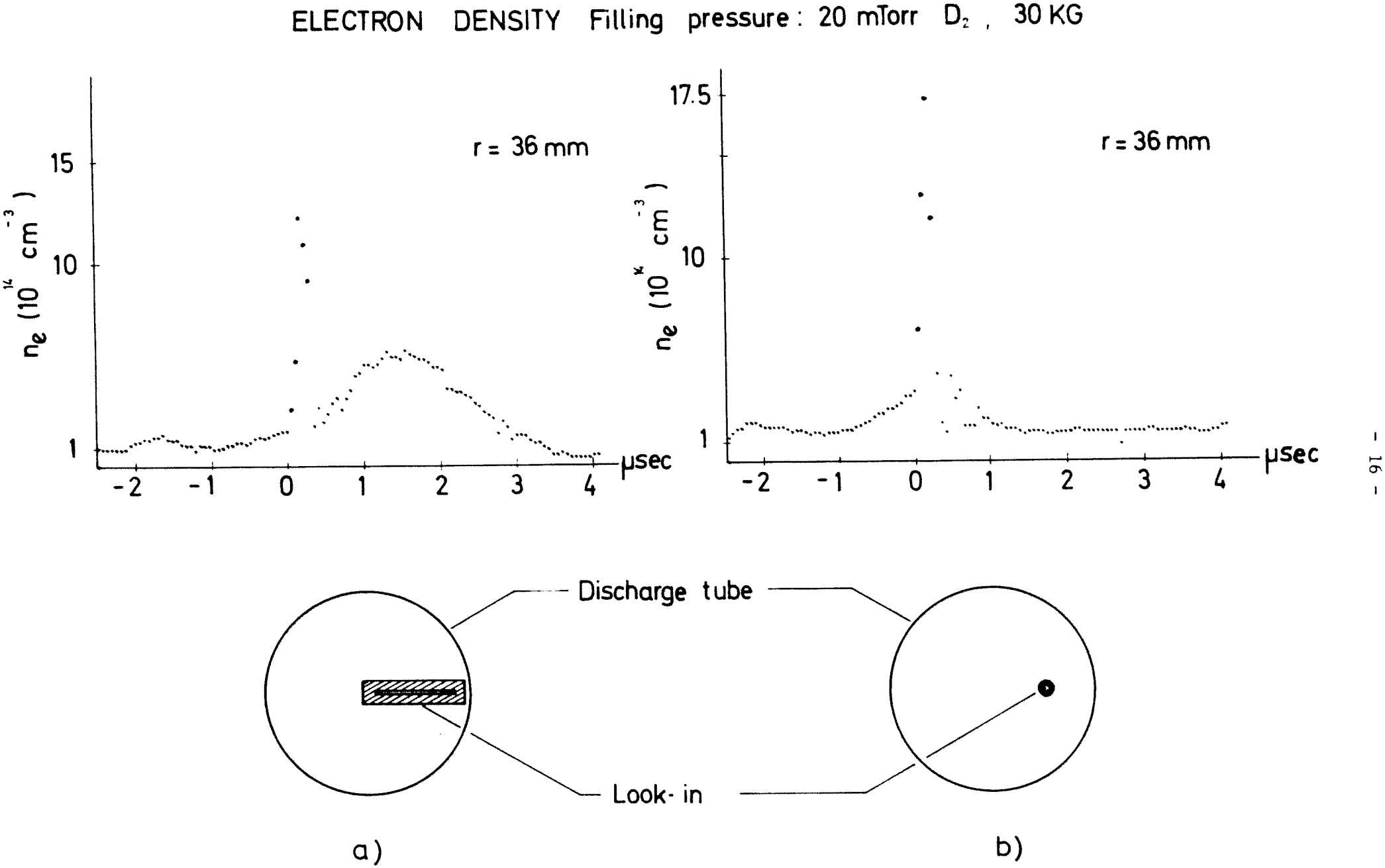
ELECTRON DENSITY Filling pressure : 20 mTorr D_2 , 30 KG
r = 36 mm
n_e (10^{14} cm^{-3})
15
10
1
-2
-1
0
1
2
3
4
μsec
r = 36 mm
n_e (10^{x} cm^{-3})
17.5
10
1
-2
-1
0
1
2
3
4
μsec
Discharge tube
Look- in
a)
b)

Figure 7

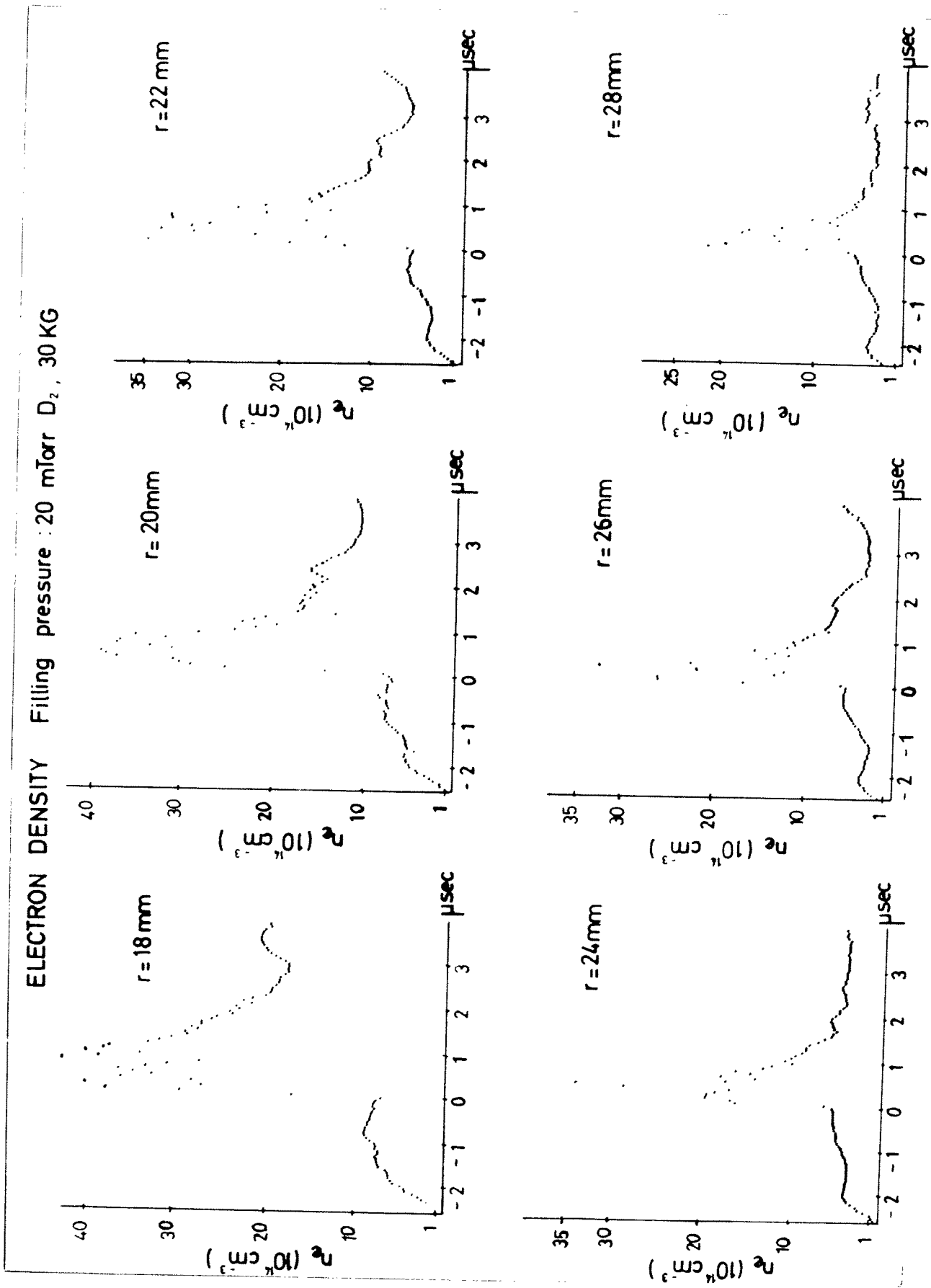
ELECTRON DENSITY Filling pressure : 20 mTorr D_2, 30 KG
r = 18 mm
r = 20mm
r = 22 mm
r = 24mm
r = 26mm
r = 28mm
n_e (10^{11} cm^{-3})
μsec

Figure 8

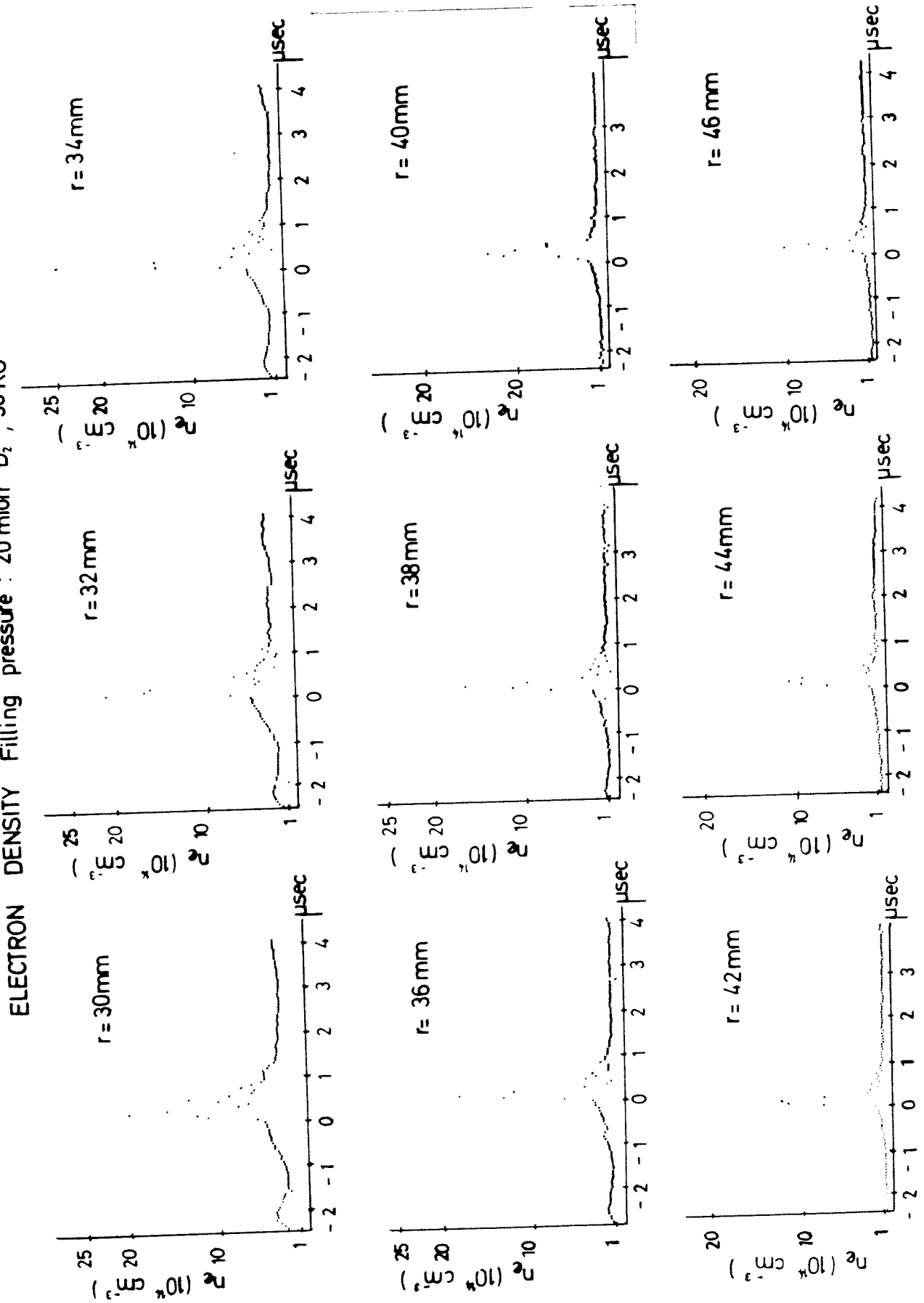
ELECTRON DENSITY Filling pressure : 20 mTorr D_2 , 30 KG
r = 30mm
r = 32mm
r = 34mm
r = 36mm
r = 38mm
r = 40mm
r = 42mm
r = 44mm
r = 46mm
n_e (10^{11} cm^{-3})
μsec

Figure 9

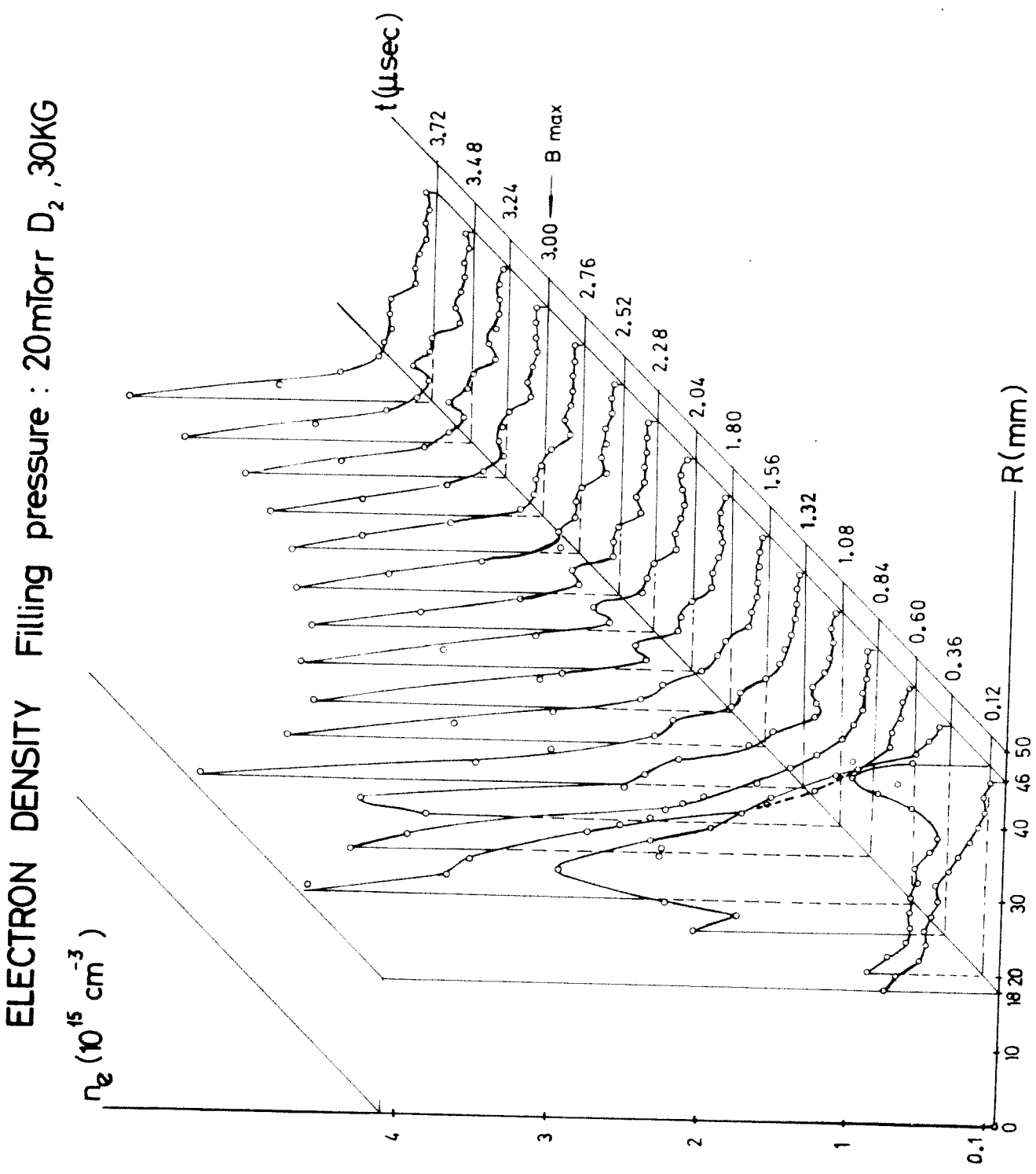
ELECTRON DENSITY Filling pressure : 20mTorr D_2 , 30KG
n_e (10^{15} cm^{-3})
t (μsec)
3.72
3.48
3.24
3.00 — B max
2.76
2.52
2.28
2.04
1.80
1.56
1.32
1.08
0.84
0.60
0.36
0.12
R (mm)
0.1
1
2
3
4
0
10
18
20
30
40
46
50

Figure 10

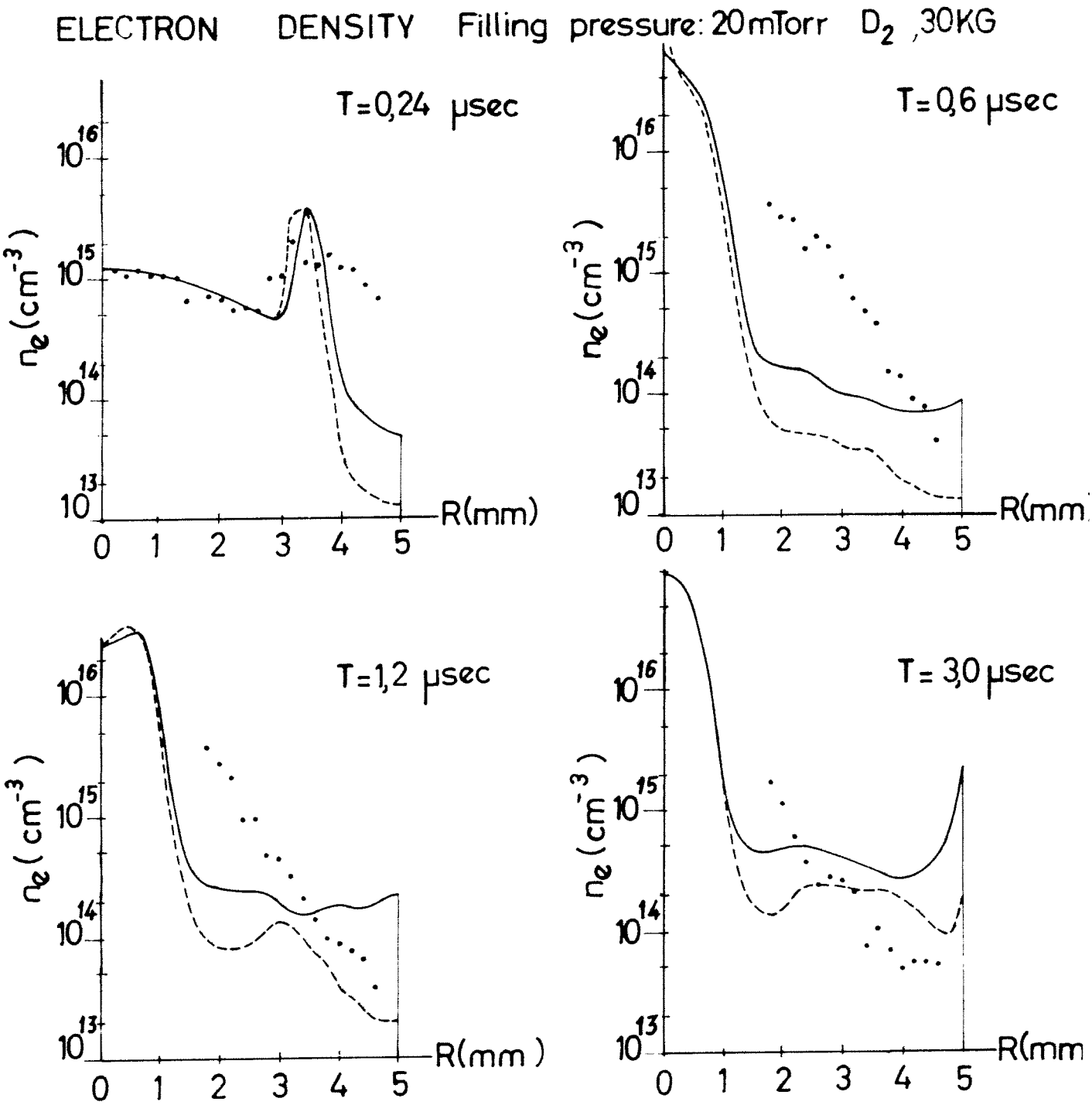
ELECTRON DENSITY Filling pressure: 20mTorr D_2 ,30KG
T=0,24 μsec
T=0,6 μsec
T=1,2 μsec
T=3,0 μsec
n_e (cm^{-3})
10^{16}
10^{15}
10^{14}
10^{13}
R(mm)
0 1 2 3 4 5

Figure 11

References

[1] Gribble R.F. et al., Proc. Second Topical Conf. on Pulsed High-Beta Plasmas, G1, (1972)

[2] Bodin H.A.B. et al., Proc. Third Conf. on Plasma Physics and Controlled Nuclear Fusion Research, Novosibirsk CN-24/K-1 (1968)

[3] Freund J. Zeitschrift für Physik, 258, 108 (1973)

[4] Jones I.R. Physical Review Letters, 28, 3, 135 (1972)

[5] Newton A.A. Culham Laboratory, Report CLM-R-62 (1966)

[6] Eberhagen A. et al., Proc. of the APS Topical Conf. on Pulsed High-Density Plasmas, LA-3770 (1967)

[7] Schumacher U., Wilhelm R., Physik Verhandlungen, Vol. 5 (1966)

[8] Niblett G.B.F., Guen T.S., Proceedings of the Phys. Society (London) 74, 737 (1959)

[9] Bodin H.A.B. et al., Plasma Physics 9, 505 (1967)

[10] Heym A. Plasma Physics 10, 1069 (1968)

[11] Herold H. et al., Los Alamos Scientific Laboratory, Report LASL 4075-MS, 69 (1968)

[12] Hofmann F. Internal Report Lausanne, LRP 46/71

[13] Schonk C.R., Morse R.L., Proc. of the APS Topical Conf. on Numerical Simulation of Plasma, LA-3990 (1968).